16 Acquaviva J, Wong R, Charest A. The multifaceted roles of the receptor tyrosine kinase ROS in development and cancer. Biochim Biophys Acta 2009;1795: 37–52.

17 Lee HJ, Seol HS, Kim JY, *et al*. ROS1 receptor tyrosine kinase, a druggable target, is frequently overexpressed in non-small cell lung carcinomas via genetic and epigenetic mechanisms. Ann Surg Oncol 2013;20: 200–208.

18 Fukui T, Ohe Y, Tsuta K, *et al*. Prospective study of the accuracy of EGFR mutational analysis by high-resolution melting analysis in small samples obtained from patients with non-small cell lung cancer. Clin Cancer Res 2008;14:4751–4757.

19 Charest A, Lane K, McMahon K, *et al*. Fusion of FIG to the receptor tyrosine kinase ROS in a glioblastoma with an interstitial del(6)(q21q21). Genes Chromosomes Cancer 2003;37:58–71.

20 Travis WD, Brambilla E, Noguchi M, *et al*. International Association for the Study of Lung Cancer/ American Thoracic Society/European Respiratory Society International multidisciplinary classification of lung adenocarcinoma. J Thorac Oncol 2011;6: 244–285.

21 Camidge DR, Kono SA, Flacco A, *et al*. Optimizing the detection of lung cancer patients harboring anaplastic lymphoma kinase (ALK) gene rearrangements potentially suitable for ALK inhibitor treatment. Clin Cancer Res 2010;16:5581–5590.

22 Yatabe Y, Matsuo K, Mitsudomi T. Heterogeneous distribution of EGFR mutations is extremely rare in lung adenocarcinoma. J Clin Oncol 2011;29: 2972–2977.

23 Stumptner-Cuvelette P, Benaroch P. Multiple roles of the invariant chain in MHC class II function. Biochim Biophys Acta 2002;1542:1–13.

24 Bruce B, Khanna G, Ren L, *et al*. Expression of the cytoskeleton linker protein ezrin in human cancers. Clin Exp Metastasis 2007;24:69–78.

25 Murakami Y, Mitsudomi T, Yatabe Y. A screening method for the ALK fusion gene in NSCLC. Front Oncol 2012;2:24.

26 Sasaki T, Koivunen J, Ogino A, *et al*. A novel ALK secondary mutation and EGFR signaling cause resistance to ALK kinase inhibitors. Cancer Res 2011;71: 6051–6060.

27 Lee J, Lee SE, Kang SY, *et al*. Identification of ROS1 rearrangement in gastric adenocarcinoma. Cancer 2013;119:1627–1635.

28 Gu TL, Deng X, Huang F, *et al*. Survey of tyrosine kinase signaling reveals ROS kinase fusions in human cholangiocarcinoma. PLoS One 2011;6:e15640.

Molecular Mechanisms Underlying Oncogenic *RET* Fusion in Lung Adenocarcinoma

Tatsuji Mizukami, MD, *† *Kouya Shiraishi, PhD,* * *Yoko Shimada, MFSc,* * *Hideaki Ogiwara, PhD,* *
Koji Tsuta, MD, PhD,‡ Hitoshi Ichikawa, PhD,§ Hiromi Sakamoto, PhD,§ Mamoru Kato, PhD,¶
Tatsuhiro Shibata, MD, PhD,¶ Takashi Nakano, MD, PhD,† and Takashi Kohno, PhD *

Background: Oncogenic *RET* fusion, caused by an inversion in chromosome 10, was recently identified as a driver mutation for the development of lung adenocarcinoma (LADC). Nevertheless, the molecular mechanism(s) underlying the rearrangement of the *RET* locus during lung carcinogenesis are unknown.

Methods: Genomic segments containing breakpoint junctions for *RET* fusions were cloned and analyzed by genomic polymerase chain reaction and genome capture sequencing using a next-generation sequencer to identify the mechanisms involved in DNA strand breaks and illegitimate joining of DNA ends. Of the 18 cases studied, 16 were identified by screening 671 LADC cases and two were previously published.

Results: Almost all (17 of 18, 94%) of the breakpoints in *RET* were located within a 2.0-kb region spanning exon 11 to intron 11 and no breakpoint occurred within 4 bp of any other. This suggested that as in papillary thyroid carcinoma, DNA strand breaks formed at nonspecific sites within this region trigger *RET* fusion. Just over half of the *RET* fusions in LADC (10 of 18, 56%) were caused by simple reciprocal inversion, and two DNA-repair mechanisms, namely nonhomologous end joining and break-induced replication, were deduced to have contributed to the illegitimate joining of the DNA ends.

Conclusions: Oncogenic *RET* fusion in LADC occurs through multiple pathways and involves the illegitimate repair of DNA strand breaks through mechanisms different from those identified in papillary thyroid carcinoma, where *RET* fusion also functions as a driver mutation.

Key Words: Lung adenocarcinoma, Molecular target therapy, Personalized medicine, *RET*, Gene fusion, DNA strand break.

(J Thorac Oncol. 2014;9: 622–630)

O ncogenic fusion of *RET* (rearranged during transfection) tyrosine kinase gene partnered with *KIF5B* (kinesin

*Division of Genome Biology, National Cancer Center Research Institute, Tokyo, Japan; †Department of Radiation Oncology, Gunma University Graduate School of Medicine, Gunma, Japan; ‡Division of Pathology and Clinical Laboratories, National Cancer Center Hospital, Tokyo, Japan; §Division of Genetics, National Cancer Center Research Institute, Tokyo, Japan; and ¶Division of Cancer Genomics, National Cancer Center Research Institute, Tokyo, Japan.

Address for correspondence: Takashi Kohno, PhD, Division of Genome Biology, National Cancer Center Research Institute, 5-1-1 Tsukiji, Chuo-ku, Tokyo 104-0045, Japan. E-mail: tkkohno@ncc.go.jp

family member 5B) and *CCDC6* (coiled-coil domain containing 6) was identified as a novel druggable driver mutation in a small subset (1–2%) of patients with lung adenocarcinoma (LADC).[1–4] Vandetanib (ZD6474) and cabozantinib (XL184), two U.S. Food and Drug Administration–approved inhibitors of the *RET* tyrosine kinase showed therapeutic responses in a few patients with *RET* fusion-positive LADC.[5,6] Several clinical trials are currently underway to examine the therapeutic effects of RET tyrosine kinase inhibitors, including these two drugs.[7,8] *RET* fusions are generated by pericentric (includes the centromere, with a breakpoint in each arm) and paracentric (not including the centromere, with both breaks in the same arm) inversions of chromosome 10 (Fig. 1*A*). As the majority of *RET* fusion-positive patients are never-smokers,[3,9,10] cigarette smoking does not cause a predisposition. Therefore, the mechanism(s) responsible for the rearrangement of the *RET* locus are unknown. Elucidation of such a mechanism(s) may help to identify risk factors that can be modified or other preventive methods that can reduce the incidence of LADC; however, no such mechanism has been identified.[8]

Analyzing the breakpoints and structural aberrations in cancer cell genomes is a powerful method of identifying the underlying molecular mechanism(s) responsible, as the breakpoints retain "traces" of the DNA strand breaks and the illegitimate joining of DNA ends.[11–13] In fact, several studies have characterized the structure of the breakpoints responsible for the *ELE1* (also known as *RFG, NCOA4,* and *ARA70*)-*RET* oncogenic fusion in cases of papillary thyroid cancer (PTC), including post-Chernobyl irradiation-induced cases, to elucidate the mechanism underlying chromosome 10 inversion generating this fusion (Fig. 1*A*).[14–17]

Here, we examined the molecular processes underlying chromosome inversions that generate oncogenic *RET* fusions in LADC by cloning genomic segments containing breakpoint junctions and by comparing their structures with those identified in PTC. The results will increase our understanding of how *RET* fusions are generated and will also have implications for diagnosis of *RET* fusion-positive LADCs.

PATIENTS AND METHODS

Patient Samples

Fourteen frozen tissues (13 surgical specimens and a pleural effusion) and two methanol-fixed paraffin-embedded tissues from surgical specimens were obtained from the
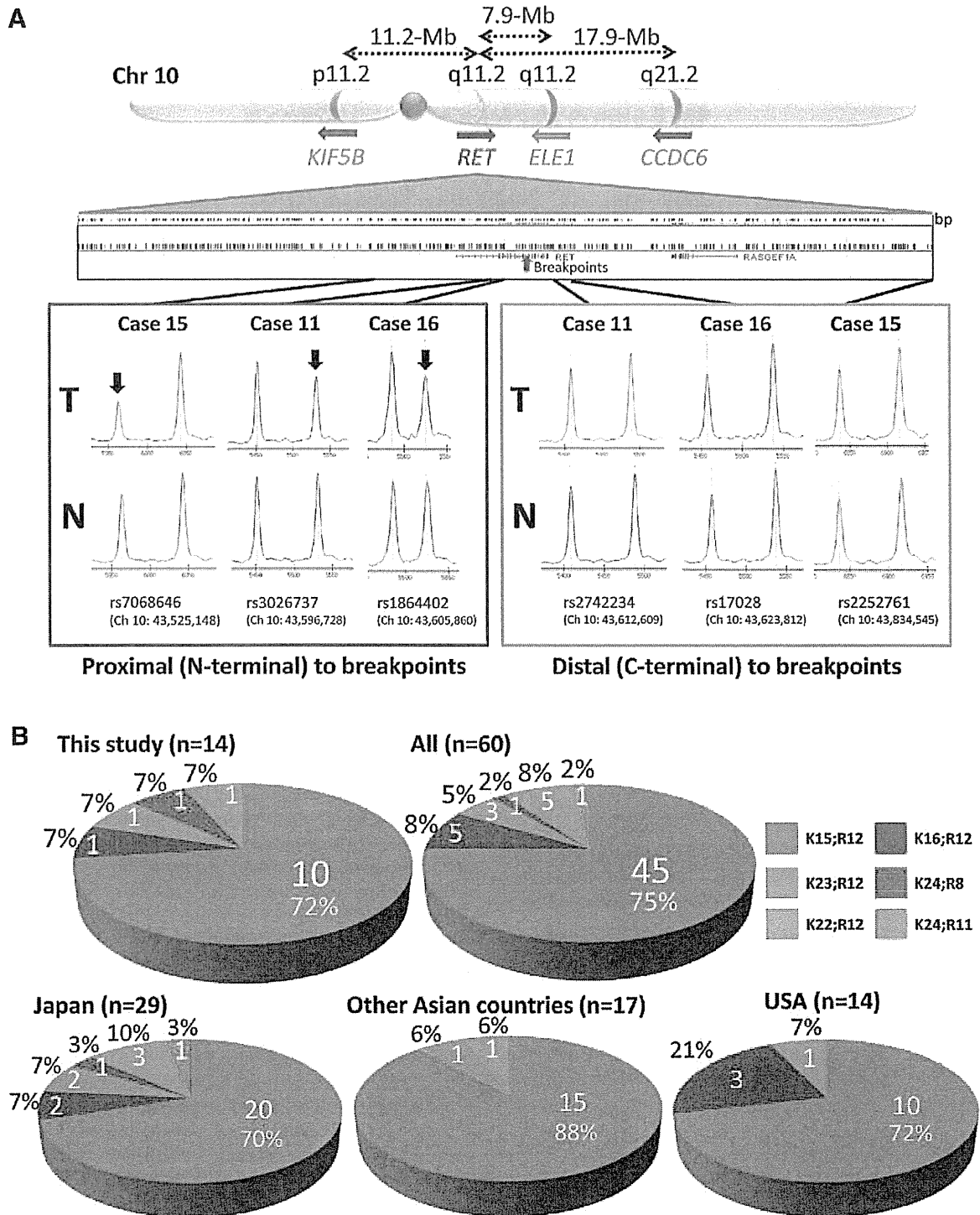
FIGURE 1. *RET* fusions. *A, Upper:* location of the *RET* oncogene and its fusion-partner genes *KIF5B, CCDC6,* and *ELE1* on chromosome 10. The *KIF5B-RET* fusion is generated in LADC, whereas the *CCDC6-RET* fusion is generated in LADC and PTC. The *ELE1-RET* fusion is frequent in radiation-induced PTC. *Lower:* LOH analysis. Allelic imbalance at SNP sites proximal and distal to the breakpoints were examined by MassArray analysis in three LADC cases with putative nonreciprocal inversions. Cases 11, 15, and 16 exhibited allelic imbalance (23%, 41%, and 29%, as indicated by arrows) at SNP loci proximal to the breakpoints, consistent with the fact that these samples have 20% to 40% tumor content. *B,* Fractions of *KIF5B-RET* fusion variants in LADCs. Fractions comprise the cohort from this study and eight published cohorts. Fractions in patients from Japan, other Asian countries (Korea and China), and the United States are shown below. LADC, lung adenocarcinoma; PTC, papillary thyroid carcinoma; LOH, loss of heterozygosity.

National Cancer Center (NCC) Biobank. These samples were from patients with LADC who received therapy at the NCC Hospital (Tokyo, Japan) between 1997 and 2012. All frozen samples were confirmed to be positive for *KIF5B-RET* fusion by reverse-transcriptase polymerase chain reaction (PCR) analysis, according to a previously described method.[3] *CCDC6-RET* fusion was detected by fusion fluorescence in situ hybridization (FISH) analysis of paraffin-embedded tissues using *RET-* and *CCDC6*-specific probes (Chromosome Science Labo Inc., Sapporo, Japan). This study was approved by the Institutional Review Board of the NCC.

Cloning and Sequencing of DNAs Containing Breakpoint Junctions

Genomic DNAs were extracted from cancer and noncancerous tissues using the QIAamp DNA Mini Kit or the QIAamp DNA Micro Kit (Qiagen, Hilden, Germany). Genomic DNA fragments containing breakpoint junctions were amplified by genomic PCR using primers that hybridized within the *KIF5B* and *RET* loci. PCR products specifically amplified in samples of interest were subjected to direct Sanger sequencing. The primers used are listed in Supplementary Table 1 (Supplementary Digital Content 1, http://links.lww.com/JTO/A541).

Genome-Capture Deep Sequencing Using a Next-Generation Speed Sequencer

Nucleotide sequences of *CCDC6-RET* fusion breakpoints were examined by targeted genome capture and massively parallel sequencing using an Ion Torrent Personal Genome Machine (Ion Torrent PGM) sequencing system and the Ion TargetSeq Custom Enrichment Kit (Life Technologies, Carlsbad, CA). One microgram of genomic DNA was subjected to enrichment using the probes listed in Supplementary Table 2 (Supplementary Digital Content 1, http://links.lww.com/JTO/A541). The mean depth of sequencing was approximately 1000.

Analysis of Sequence Reads Obtained by a Second-Generation Sequencer

Sequence reads were analyzed using a program developed by the authors. Briefly, reads were mapped to sequences of the *RET* and *CCDC6* genes using the Burrows-Wheeler Aligner, Smith-Waterman alignment (BWA-SW) software[18] to detect reads that mapped to both the *RET* and *CCDC6* genes. Breakpoints were extracted from the local alignment results of BWA-SW. The detailed procedure is described in Supplementary Notes (Supplementary Digital Content 2, http://links.lww.com/JTO/A542). Structures of breakpoint junctions were verified by Sanger sequencing of genomic PCR products.

Loss of Heterozygosity Analysis

Genomic DNAs obtained from cancerous and noncancerous tissues were subjected to single nucleotide polymorphism (SNP) genotyping using the Illumina HumanOmni1 2.5M Chip (Illumina, San Diego, CA). Based on the B-allele frequencies obtained using the Illumina GenomeStudio software, loss of heterozygosity (LOH) regions in *RET* and surrounding regions were deduced. Representative SNP loci were subjected to analysis of allelic imbalance using the Sequenom MassARRAY system (Sequenom, San Diego, CA).

Analysis of Nucleotide Sequences

Nucleotide sequence analysis, including search for sequence homology, was performed using the Genetyx-SV/RC Ver 8.0.1. software (Genetyx, Tokyo, Japan). Information about the distribution of repetitive elements, GC contents, conservation, DNA methylation, DNase sensitivity, and histone modification within the *RET* gene was obtained using the UCSC genome browser (http://genome.ucsc.edu/cgi-bin/hgGateway).

RESULTS

KIF5B-RET Fusion Variations in LADC

In our previous study, six of 319 LADC cases (1.9%) carried *KIF5B-RET* fusions.[3] In this study, we examined *KIF5B-RET* fusion by reverse-transcriptase PCR in a further 352 LADC cases and found eight additional *KIF5B-RET* fusion-positive cases. In total, 14 of 671 cases (2.1%) were positive for *KIF5B-RET* fusions (cases 1–4 and 7–16 in Table 1 and Supplementary Table 3, Supplementary Digital Content 1, http://links.lww.com/JTO/A541), and this frequency was consistent with those reported for other cohorts.[9,10,19]

Among those 14 cases, 10 (71%) contained a fusion of *KIF5B* exon 15 to *RET* exon 12 (K15;R12), whereas the remaining four each contained other variants. Thus, K15;R12 is the most frequent variant (Fig. 1B). The prevalence of the K15;R12 variant (45 of 60, 75%) was verified in a total of 60 cases, including 46 cases from eight other cohorts published to date[1–4,9,10,19,20] (Fig. 1B, Supplementary Table 4, Supplementary Digital Content 1, http://links.lww.com/JTO/A541). This preference was similar among cohorts from Japan, other Asian countries, and the United States ($p > 0.05$ by Fisher's exact test).

Distribution of Breakpoints in the *RET* and *KIF5B* Genes

To explore the molecular processes underlying *RET* fusion in LADC, we examined the location (clustering) of the breakpoints and the structure of the breakpoint junctions; information about the former enabled us to deduce the genomic or chromosomal features that make DNA susceptible to strand breaks, whereas information about the latter enabled us to deduce the mechanism underlying the illegitimate joining of DNA ends by DNA repair pathways.

The locations of the 28 breakpoints in the 14 *KIF5B-RET* fusion-positive cases mentioned above were identified by Sanger sequencing analysis of genomic PCR products and mapped (yellow arrowheads in Fig. 2A and B). The breakpoints in a single Korean case from another study were also identified and mapped (orange arrowheads in Fig. 2A; case 17 in Table 1). Consistent with the predominance of K15;R12 variants, most of the breakpoints were mapped to intron 11 of *RET* and intron 15 of *KIF5B* (Fig. 2, detailed information in Supplementary Table 5, Supplementary Digital Content 1, http://links.lww.com/JTO/A541).

TABLE 1. Structure of Breakpoint Junctions of *RET* Fusions in Lung Adenocarcinoma

No.	Sample Name	Fusion Partner	Reciprocal/ Nonreciprocal	Deletion in the Joining		DNA Segment Duplication by Inversion		Nucleotide Overlap at Junction		Nucleotide Insertion at Junction		Mode of DNA End Joining	LOH Proximal to *RET*	Smoking
				RET	Partner	*RET*	Partner	Partner -*RET*	*RET*-Partner	Partner -*RET*	*RET*-Partner			
1	BR0020	*KIF5B*	Reciprocal	—	—	—	—	—	—	—	—	NHEJ	NT	No
2	L07K201T	*KIF5B*	Reciprocal	14 bp	19 bp	—	—	C	—	—	ATA	NHEJ	NT	Yes
3	349T	*KIF5B*	Reciprocal	1 bp	7 bp	—	—	—	—	A	A	NHEJ	NT	Yes
4	AD08-341T	*KIF5B*	Reciprocal	16 bp	26 bp	—	—	—	—	—	—	NHEJ	NT	No
5	RET-030	*CCDC6*	Reciprocal	52 bp	1021 bp	—	— —	—		—	—	NHEJ	NT	No
6	RET-024	*CCDC6*	Reciprocal	14 bp	2 bp	—	—	—	—	—	—	NHEJ	NT	Yes
7	AD12-106T	*KIF5B*	Reciprocal	—	573 bp	490 bp	—	—	—	—	—	BIR	NT	Yes
8	BR0030	*KIF5B*	Reciprocal	—	—	—	211 bp	—	—	—	—	BIR	NT	No
9	442T	*KIF5B*	Reciprocal	269 bp	—	—	232 bp	—	—	—	—	BIR	NT	No
10	AD08-144T	*KIF5B*	Reciprocal	5 bp	—	—	33 bp	—	—	—	—	BIR	NT	No
11	BR1001	*KIF5B*	Nonreciprocal					—		AGT		NHEJ	+	No
12	AD09-369T	*KIF5B*	Nonreciprocal					CTC		—		NHEJ (alternative end joining)	NT	No
13	BR1002	*KIF5B*	Nonreciprocal					A		—		NHEJ	NT	No
14	AD12-001T	*KIF5B*	Nonreciprocal					—		—		NHEJ	NT	Yes
15	BR1003	*KIF5B*	Nonreciprocal					—		CTTT		NHEJ	+	No
16	BR1004	*KIF5B*	Nonreciprocal					—		RET exon 7 to intron 7 (359 bp)		Complex rearrange	+	No
17	AK55[a]	*KIF5B*	Nonreciprocal					—		GT		NHEJ	NT	No
18	LC-2/ad[b]	*CCDC6*	Nonreciprocal					—		—		NHEJ	NT	Unknown

[a]Ju et al.[4]
[b]Suzuki et al.[21]
LOH, loss of heterozygosity; NHEJ, nonhomologous end joining; NT, not tested; BIR, break-induced replication; blank, not applicable.
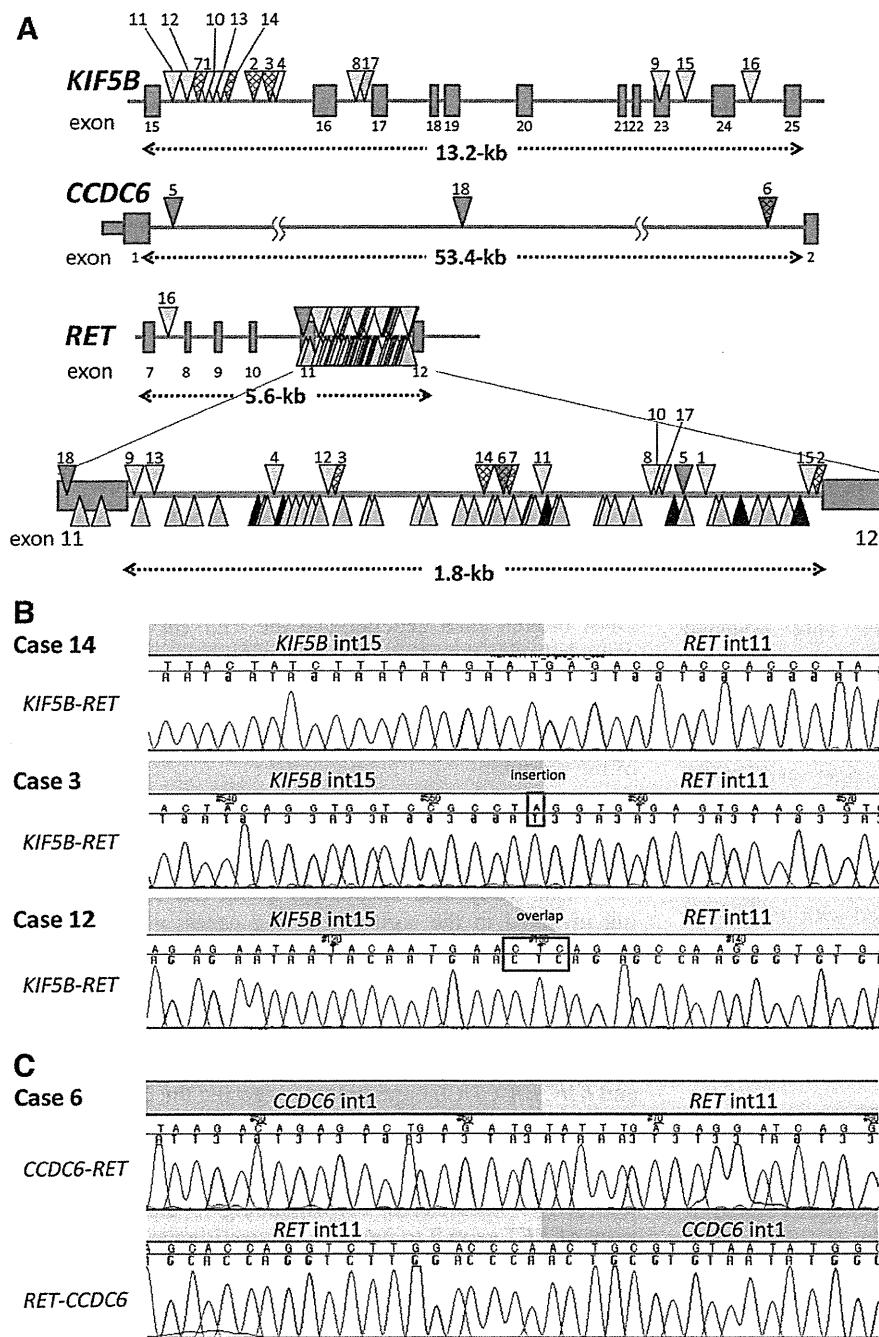
FIGURE 2. Breakpoint analysis. *A*, Distribution of breakpoints in the *CCDC6*, *KIF5B*, and *RET* genes. Yellow arrowheads indicate the locations of breakpoints for *KIF5B-RET* fusions in Japanese cases (cases 1–4 and 7–16 in Table 1), whereas the orange arrowhead indicates the breakpoints in a single Korean case (case 17). Green arrowheads indicate the locations of breakpoints of *CCDC6-RET* fusions in three Japanese cases (cases 5, 6, and 18). Arrowheads for ever-smoker LADC cases are hatched. Gray and black arrowheads indicate breakpoints of *RET-ELE1* fusion in 38 radiation-induced post-Chernobyl PTCs and six sporadic PTCs, respectively.[14–17] *B*, Electropherograms for Sanger sequencing of genomic fragments encompassing *KIF5B-RET* breakpoint junctions. PCR products were directly sequenced. Examples of three fusion patterns (joined without any nucleotide insertions or overlaps, joined with a nucleotide insertion, and joined with three nucleotide overlap) are shown. Inserted and overlapping nucleotides at breakpoint junctions are indicated, respectively, by the blue and red boxes. *C*, Electropherogram for Sanger sequencing of genomic fragments encompassing *CCDC6-RET* and *RET-CCDC6* breakpoint junctions. LDAC, lung adenocarcinoma; PCR, polymerase chain reaction; PTC, papillary thyroid carcinoma.

None of the *RET* and *KIF5B* breakpoints mapped at the same position, and no breakpoint was within 6 bp of another. To further investigate the breakpoint clustering, we mapped breakpoints in three cases of *CCDC6-RET* fusion, a minor fusion variant (cases 5, 6, and 18 in Table 1 and Supplementary Table 3, Supplementary Digital Content 1, http://links.lww.com/JTO/A541). Two of these cases were primary tumors, diagnosed by break apart and fusion *FISH*, and their breakpoints were determined by genome-capture deep sequencing of genomic DNAs using a second-generation sequencer. The remaining case was a LADC cell line from a Japanese patient, for which the breakpoints had previously been determined by the same method.[21] Two breakpoints and one breakpoint in the *RET* gene were mapped to intron 11 and exon 11, respectively (green arrowheads in Fig. 2), and no breakpoint was located within 5 bp of another. In total, a 2.0-kb region spanning exon 11 to intron 11 of *RET* and a 5.6-kb region spanning intron 15 of *KIF5B* (10 of 15, 75%) contained the majority of breakpoints (17 of 18 [94%] and 10 of 15 [75%], respectively), and these breakpoints

626

were at least 5 bp from each other. Breakpoints within exon 11 to intron 11 of RET and intron 15 of KIF5B were not distributed in an evidently biased manner, nor did they exhibit any particular nucleotide sequence or composition (Supplementary Table 5, Supplementary Digital Content 1, http://links.lww.com/JTO/A541). Therefore, DNA strand breaks triggering oncogenic RET fusions in LADC occur preferentially in a few defined regions, but at nonspecific sites within those regions.

Reciprocal and Nonreciprocal Inversions Causing RET Fusions

To explore the modes of DNA end joining that give rise to RET fusion, we investigated the structures of RET fusion breakpoint junctions. To address whether chromosome inversion events were reciprocal, we cloned genomic segments containing reciprocal breakpoint junctions (i.e., RET-KIF5B and RET-CCDC6) from 17 Japanese cases (Table 1). Ten of the 17 cases, consisting of eight KIF5B-RET and two CCDC6-RET cases, allowed amplification of reciprocal genomic segments using PCR primers set 1 kb away from the identified KIF5B-RET or CCDC6-RET breakpoints. This indicated that these fusions were the results of simple reciprocal inversions (cases 1–10 in Table 1, Fig. 2C). On the other hand, the remaining seven cases did not allow amplification of genomic segments encompassing the reciprocal breakpoint junctions (cases 11–16 and 18 in Table 1). Three of these seven cases, for which corresponding noncancerous DNA was available, were subjected to LOH analysis at the RET locus. LOH was detected at a region proximal (N-terminal) to the breakpoints in all three cases (cases 11, 15, and 16 in Table 1, Fig. 1A), indicating nonreciprocal inversion associated with deletion of a copy of the region proximal to the breakpoints. In addition, the inversion in the aforementioned Korean case (case 17) is also nonreciprocal.[4] These data suggested that only a fraction of RET fusions (10 of 18, 56%) are caused by simple reciprocal inversions.

Modes of DNA End Joining That Give Rise to Reciprocal Inversions

Two major types of DNA repair pathways cause structural variations.[11,12] The first type is nonhomologous end joining (NHEJ) of DNA double strand breaks (DSBs), which requires very short (a few base pairs) or no homology, and often inserts a few nucleotides at breakpoint junctions.[8,22,23] NHEJ has canonical and noncanonical forms; in the latter, called alternative end joining, DNA ends are joined using microhomology of a few nucleotides at breakpoints.[24] The second type includes repair pathways that use long (>10 bp) homology at DNA ends, such as break-induced replication (BIR) and nonallelic homologous recombination.[12,25]

Sequence analysis of breakpoint-containing genomic segments in 10 reciprocal cases revealed that deletions frequently (8 of 10, 80%) occur in RET and/or its partner locus (i.e., KIF5B or CCDC6) upon DNA end joining (Table 1). This analysis also enabled us to deduce that both types of repair pathways described above are involved in these joining events. In six of the cases (cases 1–6 in Table 1), four DNA ends were joined, and in two cases, insertions were observed (representative cases in Supplementary Fig. 1, Supplementary Digital Content 3, http://links.lww.com/JTO/A543). The lack of significant homology between the sequences of the RET and KIF5B/CCDC6 breakpoints led us to deduce that DNA end joining was mediated by NHEJ in these six cases: two DSBs formed, one each in RET and its partner locus, and the four resultant DNA ends were illegitimately joined by canonical or noncanonical NHEJ (Fig. 3A).

The remaining four cases (cases 7–10 in Table 1) had a distinctive feature. DNA segments of 33 to 490 bp from either the RET or KIF5B locus were retained at both the KIF5B-RET and RET-KIF5B breakpoints, resulting in duplication of these segments. Notably, two regions encompassing the breakpoint in a locus exhibited sequence homology to the duplicated segment of the other locus (representative cases in Supplementary Fig. 2, Supplementary Digital Content 3, http://links.lww.com/JTO/A543). This feature led us to deduce that these joining events were mediated by BIR, using both DNA ends generated by DNA single-strand breaks at the RET or fusion-partner locus (Fig. 3B). Specifically, two DNA broken ends generated at the RET (or partner locus) annealed with the DSB sites of the fusion-partner (or RET) locus through sequence homology and were then subjected to ectopic DNA replication. This process left the same DNA segment at both breakpoint junctions, resulting in duplication of the segment.

Speculated Mode of DNA End Joining Giving Rise to Nonreciprocal Inversion

Our study also speculated about the modes of joining involved in the eight remaining cases, which were not likely to have been subjected to simple reciprocal inversion and are therefore defined here as nonreciprocal (cases 11–18 in Table 1). Due to the lack of sequence information from breakpoints in reciprocal counterparts, deletions could not be assessed. The lack of significant homology between the RET and KIF5B/CCDC6 breakpoints suggested the involvement of NHEJ. Consistent with this idea, insertion of a few nucleotides, a common trace of NHEJ, was observed in three cases (cases 11, 15, and 17). A single case (case 16) had an insertion of 349 nucleotides, corresponding to the inverted segment of RET exon 7 to intron 7, suggesting the occurrence of an unspecified complex rearrangement mediated by a process other than NHEJ, such as fork stalling and template switching (Lee et al., 2007). These results suggest that the predominant molecular process is illegitimate NHEJ repair, in which two DSBs are formed both in the RET and partner loci, and one end of the partner locus (the N-terminal part of KIF5B or CCDC6) and one end of the RET locus (the C-terminal part) are joined by NHEJ. Nevertheless, the remaining two DNA ends were not joined in a simple manner. DNA segments within the DNA ends were either lost or joined with DNA ends other than those at the RET, KIF5B, and CCDC6 loci, consistent with the observations of LOH at regions proximal to breakpoints in RET (Table 1). In fact, in case 17, the 3′ part of the KIF5B gene was fused to the KIAA1462 gene, 2.0 Mb away from KIF5B.[4]
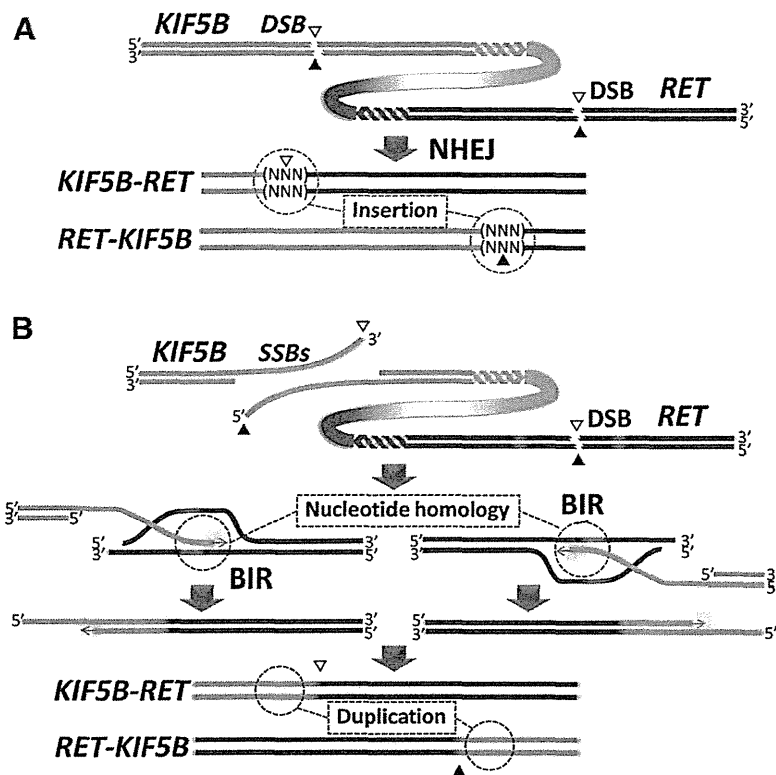
FIGURE 3. Deduced processes of reciprocal inversion by NHEJ and BIR. A, NHEJ. Four DNA ends generated by DSBs at RET and a partner locus were directly joined. Often, insertions of nucleotides (NNN) at breakpoint junctions are observed. B, BIR. Here, DNA single-strand breaks (SSBs) occur in the KIF5B locus and a DSB occurs in the RET locus. The two SSBs at the KIF5B locus trigger BIR by annealing at two homologous sites in the RET locus. BIR results in duplication of a KIF5B segment. As a result, the RET breakpoints in the KIF5B-RET and RET-KIF5B fusions are located at the same position (a DSB site), whereas the KIF5B breakpoints in these fusions are located at different positions (two SSB sites). ▽, breakpoints for partner-RET fusion; ▲, breakpoints for RET-partner fusion. NHEJ, nonhomologous end joining; BIR, break-induced replication.

DISCUSSION

In this study, we investigated the molecular mechanisms underlying oncogenic RET fusion in LADCs. Distribution of breakpoints made us consider a 2.0-kb segment spanning RET exon 11 to intron 11 (and also a 5.6-kb segment spanning KIF5B intron 15) as a breakpoint cluster region(s). The breakpoints in these regions were dispersed at intervals larger than 4 bp. The inferred breakpoints do not necessarily indicate the sites of actual DNA breaks because resection of nucleotides from DNA ends sometimes occurs during the DNA repair.[23] In fact, we observed nucleotide deletions in eight of 10 LADC cases with reciprocal KIF5B/CCDC6-RET inversions. Nevertheless, when the locations of putative breakpoints before DNA end resection were included, the breakpoint distribution remained scattered. These data strongly suggested that the majority of DNA breaks triggering RET fusions occur at nonspecific sites in defined regions of a few kb in size. Furthermore, this seems to hold true irrespective of etiology and tumor type: the distribution of breakpoints was not significantly different between ever- and never-smokers, and RET exon 11 to intron 11 was also defined as a breakpoint cluster region for RET fusions in PTCs, as previously reported.[14–17] The cases shown in Figure 2 (gray and black arrowheads) include PTCs induced by post-Chernobyl irradiation, in which DNA breaks were presumably caused exclusively by irradiation; the random breakpoint distributions in these PTCs were similar to those of the LADCs we analyzed.

We investigated the DNA end-joining pathways that gave rise to RET fusions by analyzing the structures of breakpoint junctions. NHEJ was found to be one of the major pathways of DNA

end joining. We and others also showed that NHEJ is also prominently involved in interstitial deletions that inactivate tumor-suppressor genes, such as CDKN2A/p16 and STK11/LKB1, in lung cancer.[13,26,27] Thus, NHEJ contributes to the occurrence of driver mutations in both tumor-suppressor genes and oncogenes during lung carcinogenesis. Our data also reveal a possible contribution of BIR in DNA end joining to generate reciprocal inversions. We deduced that BIR occurred from DNA ends, probably generated by DNA single-strand breaks, in the RET or partner locus, beginning with annealing with the other locus through nucleotide homologies of tens to hundreds of base pairs. This process resulted in duplication of breakpoint-flanking DNA segments of tens to hundreds of base pairs. BIR has recently been implicated in oncogenic RAF fusions in pediatric brain tumors.[28] In those cases, the sequence homology used for annealing of DNA ends was on the order of a few base pairs. Thus, BIR might generate oncogenic fusions frequently, although the detailed process may differ according to tumor type.

Irrespective of the similarities in breakpoint distribution, several processes involved in RET fusions differed between LADC and PTC (Fig. 4). Reciprocal inversion was unlikely to have occurred by BIR in PTC because none of the PTC cases exhibited the duplication of DNA segments that were observed in LADC; therefore, the joining of DNA ends in PTC was likely to have been mediated exclusively by NHEJ.[17] This is plausible because RET fusions preferentially occur in PTCs in patients suffering from high-dose radiation exposure, suggesting that DSBs generated at the RET or partner loci triggered the chromosome rearrangements that generated RET fusions.[29] Repetitive NHEJ repair of abundant

FIGURE 4. Molecular processes underlying *RET* gene fusions in LADC and PTC. Different processes are involved in *RET* fusion in different tumor types. Both reciprocal and nonreciprocal inversions occur in LADC. In LADC, BIR and NHEJ are responsible for DNA end joining in reciprocal inversion, whereas NHEJ is exclusively involved in nonreciprocal inversion. In PTC, reciprocal inversion by NHEJ is dominant. LADC, lung adenocarcinoma; PTC, papillary thyroid carcinoma; NHEJ, nonhomologous end joining; BIR, break-induced replication.
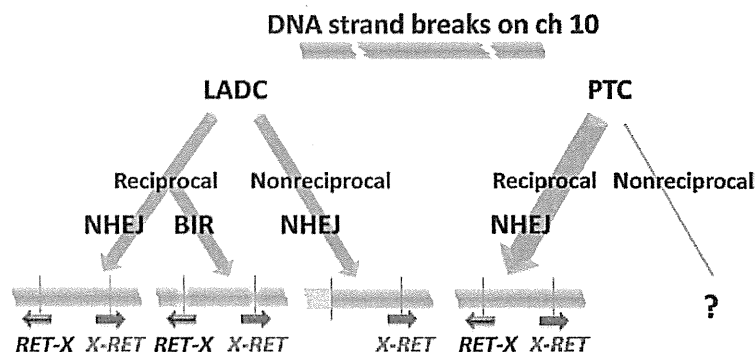
DSBs, which occurs in the context of irradiation, may increase the likelihood of illegitimate repair generating *RET* fusion. On the other hand, in LADC, both DSBs and single-strand breaks formed by multiple causes might trigger rearrangements by multiple DNA repair pathways. The high frequency of nonreciprocal inversion also distinguishes LADC from PTC, for previous study revealed that *RET* fusions result from reciprocal inversion in most cases (43 of 47, 91%).[14,15] Frequent nonreciprocal inversion is consistent with the observation that *KIF5B-RET* fusion-positive tumors contain deletions of the 5′ part of *RET*, as revealed by FISH staining patterns.[1] The present study provides a molecular basis for such a distinct FISH finding and will help to define the criteria used to diagnose *RET*-fusion-positive LADC. Interestingly, FISH analysis also revealed that another driver mutation, *EML4-ALK* fusion, in LADC, caused by a paracentric inversion of chromosome 2, also involves deletion of the 5′ region of the *ALK* oncogene locus.[30,31] Although the structures of breakpoint junctions of *ALK* fusions have not been characterized to the best of our knowledge, these results indicate that a significant fraction of chromosome inversions that cause oncogenic fusions in lung cancer are likely to be nonreciprocal.

Finally, a few issues remain to be elucidated regarding the molecular processes generating oncogenic *RET* fusions. First, although this and previous PTC studies imply that the 2.0-kb region spanning the *RET* exon 11 to intron 11 region is susceptible to DNA strand breaks, the underlying mechanisms remain unknown. For, this region does not exhibit distinctive features known to make DNA susceptible to breaks (Supplementary Fig. 3, Supplementary Digital Content 3, http://links.lww.com/JTO/A543; details in Supplementary Notes, Supplementary Digital Content 2, http://links.lww.com/JTO/A542). Second, the etiological factors that cause DNA strand breaks, and the factors that determine reciprocal or nonreciprocal inversion and selection of DNA repair pathways, also remain unknown. The mode of joining and breakpoint distribution was irrespective of smoking history, and therefore, DNA damage due to smoking is unlikely to be an important factor. The fact that *RET* fusions are more frequent in LADC of never-smokers than in that of ever-smokers indicates that undefined etiological factors play major roles in the occurrence of *RET* fusions.

ACKNOWLEDGMENTS

REFERENCES

1. Takeuchi K, Soda M, Togashi Y, et al. RET, ROS1 and ALK fusions in lung cancer. *Nat Med* 2012;18:378–381.
2. Lipson D, Capelletti M, Yelensky R, et al. Identification of new ALK and RET gene fusions from colorectal and lung cancer biopsies. *Nat Med* 2012;18:382–384.
3. Kohno T, Ichikawa H, Totoki Y, et al. KIF5B-RET fusions in lung adenocarcinoma. *Nat Med* 2012;18:375–377.
4. Ju YS, Lee WC, Shin JY, et al. A transforming KIF5B and RET gene fusion in lung adenocarcinoma revealed from whole-genome and transcriptome sequencing. *Genome Res* 2012;22:436–445.
5. Gautschi O, Zander T, Keller FA, et al. A patient with lung adenocarcinoma and RET fusion treated with vandetanib. *J Thorac Oncol* 2013;8:e43–e44.
6. Drilon A, Wang L, Hasanovic A, et al. Response to Cabozantinib in patients with RET fusion-positive lung adenocarcinomas. *Cancer Discov* 2013;3:630–635.
7. Kohno T, Tsuta K, Tsuchihara K, Nakaoku T, Yoh K, Goto K. RET fusion gene: translation to personalized lung cancer therapy. *Cancer Sci* 2013;104:1396–1400.
8. Shaw AT, Hsu PP, Awad MM, Engelman JA. Tyrosine kinase gene rearrangements in epithelial malignancies. *Nat Rev Cancer* 2013;13:772–787.
9. Wang R, Hu H, Pan Y, et al. RET fusions define a unique molecular and clinicopathologic subtype of non-small-cell lung cancer. *J Clin Oncol* 2012;30:4352–4359.
10. Suehara Y, Arcila M, Wang L, et al. Identification of KIF5B-RET and GOPC-ROS1 fusions in lung adenocarcinomas through a comprehensive mRNA-based screen for tyrosine kinase fusions. *Clin Cancer Res* 2012;18:6599–6608.
11. Yang L, Luquette LJ, Gehlenborg N, et al. Diverse mechanisms of somatic structural variations in human cancer genomes. *Cell* 2013;153:919–929.
12. Gu W, Zhang F, Lupski JR. Mechanisms for human genomic rearrangements. *Pathogenetics* 2008;1:4.
13. Kohno T, Yokota J. Molecular processes of chromosome 9p21 deletions causing inactivation of the p16 tumor suppressor gene in human cancer: deduction from structural analysis of breakpoints for deletions. *DNA Repair (Amst)* 2006;5:1273–1281.

14. Nikiforov YE, Koshoffer A, Nikiforova M, Stringer J, Fagin JA. Chromosomal breakpoint positions suggest a direct role for radiation in inducing illegitimate recombination between the ELE1 and RET genes in radiation-induced thyroid carcinomas. *Oncogene* 1999;18:6330–6334.

15. Bongarzone I, Butti MG, Fugazzola L, et al. Comparison of the breakpoint regions of ELE1 and RET genes involved in the generation of RET/PTC3 oncogene in sporadic and in radiation-associated papillary thyroid carcinomas. *Genomics* 1997;42:252–259.

16. Minoletti F, Butti MG, Coronelli S, et al. The two genes generating RET/PTC3 are localized in chromosomal band 10q11.2. *Genes Chromosomes Cancer* 1994;11:51–57.

17. Klugbauer S, Pfeiffer P, Gassenhuber H, Beimfohr C, Rabes HM. RET rearrangements in radiation-induced papillary thyroid carcinomas: high prevalence of topoisomerase I sites at breakpoints and microhomology-mediated end joining in ELE1 and RET chimeric genes. *Genomics* 2001;73:149–160.

18. Li H, Durbin R. Fast and accurate long-read alignment with Burrows-Wheeler transform. *Bioinformatics* 2010;26:589–595.

19. Cai W, Su C, Li X, et al. KIF5B-RET fusions in Chinese patients with non-small cell lung cancer. *Cancer* 2013;119:1486–1494.

20. Yokota K, Sasaki H, Okuda K, et al. KIF5B/RET fusion gene in surgically-treated adenocarcinoma of the lung. *Oncol Rep* 2012;28:1187–1192.

21. Suzuki M, Makinoshima H, Matsumoto S, et al. Identification of a lung adenocarcinoma cell line with CCDC6-RET fusion gene and the effect of RET inhibitors in vitro and in vivo. *Cancer Sci* 2013;104:896–903.

22. Mahaney BL, Meek K, Lees-Miller SP. Repair of ionizing radiation-induced DNA double-strand breaks by non-homologous end-joining. *Biochem J* 2009;417:639–650.

23. Lieber MR. The mechanism of double-strand DNA break repair by the nonhomologous DNA end-joining pathway. *Annu Rev Biochem* 2010;79:181–211.

24. Bennardo N, Cheng A, Huang N, Stark JM. Alternative-NHEJ is a mechanistically distinct pathway of mammalian chromosome break repair. *PLoS Genet* 2008;4:e1000110.

25. Lee JA, Carvalho CM, Lupski JR. A DNA replication mechanism for generating nonrecurrent rearrangements associated with genomic disorders. *Cell* 2007;131:1235–1247.

26. Sasaki S, Kitagawa Y, Sekido Y, et al. Molecular processes of chromosome 9p21 deletions in human cancers. *Oncogene* 2003;22:3792–3798.

27. Matsumoto S, Iwakawa R, Takahashi K, et al. Prevalence and specificity of LKB1 genetic alterations in lung cancers. *Oncogene* 2007;26:5911–5918.

28. Lawson AR, Hindley GF, Forshew T, et al. RAF gene fusion breakpoints in pediatric brain tumors are characterized by significant enrichment of sequence microhomology. *Genome Res* 2011;21:505–514.

29. Hamatani K, Eguchi H, Ito R, et al. RET/PTC rearrangements preferentially occurred in papillary thyroid cancer among atomic bomb survivors exposed to high radiation dose. *Cancer Res* 2008;68:7176–7182.

30. Dai Z, Kelly JC, Meloni-Ehrig A, et al. Incidence and patterns of ALK FISH abnormalities seen in a large unselected series of lung carcinomas. *Mol Cytogenet* 2012;5:44.

31. Yoshida A, Tsuta K, Nitta H, et al. Bright-field dual-color chromogenic in situ hybridization for diagnosing echinoderm microtubule-associated protein-like 4-anaplastic lymphoma kinase-positive lung adenocarcinomas. *J Thorac Oncol* 2011;6:1677–1686.